29. Golts N, Snyder H, Frasier M, Theisler C, Choi P, Wolozin B. Magnesium inhibits spontaneous and iron-induced aggregation of alpha-synuclein. *J Biol Chem* 2002; **277**: 16116–16123.
30. Roos RA, Bots GT, Hermans J. Neuronal nuclear membrane indentation and astrocyte/neuron ration in Huntington's disease. A quantitative electron microscopic study. *J Hirnforsch* 1985; **26**: 689–693.
31. Takahashi H, Egawa S, Piao YS *et al.* Neuronal nuclear alteration in dentatorubural-pallidoluysian atrophy: ultrastructural and morphometric studies of the cerebellar granule cells. *Brain Res* 2001; **919**: 12–19.
32. Parent A. Substantia nigra. Chapter 14: Midbrain. In: *Carpenter's Human Neuroanatomy*, 9th edn. Media: Williams & Wilkins, 1996; 557–568
33. Yanagihara R, Garruto RM, Gajdusek DC *et al.* Calcium and vitamin D metabolism in Guamanian Chamorros with amyotrophic lateral sclerosis and parkinsonism–dementia. *Ann Neurol* 1984; **15**: 42–48.
34. Ahlskog JE, Waring SC, Kurland LT *et al.* Guamanian neurodegenerative diseases: calcium metabolism/heavy metal hypothesis. *Neurology* 1995; **45**: 1340–1344.
35. Oyanagi K, Makifuchi T, Ohtoh T *et al.* Amyotrophic lateral sclerosis of Guam: the nature of the neuropathological findings. *Acta Neuropathol* 1994; **88**: 405–412.

Appendix I Number of examined rats in each experimental group

Groups from exposure period	Groups of food	Gender	Examined no. rats
i	#1	Fetus & New born	8
		Male	4
		Female	4
	#2	Fetus & New born	8
		Male	3
		Female	7
	#3	Fetus & New born	9
		Male	5
		Female	6
	#4	Fetus & New born	13
		Male	4
		Female	4
	#5	Fetus & New born	7
		Male	4
		Female	7
	#6	Fetus & New born	8
		Male	6
		Female	5
ii	#1	Fetus & New born	8
		Male	4
		Female	6
	#2	Fetus & New born	8
		Male	5
		Female	6
	#3	Fetus & New born	9
		Male	10
		Female	8
	#4	Fetus & New born	13
		Male	10
		Female	16
	#5	Fetus & New born	7
		Male	6
		Female	6
	#6	Fetus & New born	8
		Male	4
		Female	6
iii	#1	Fetus & New born	8
		Male	3
		Female	7
	#2	Fetus & New born	8
		Male	6
		Female	6

Appendix I *Continued*

Groups from exposure period	Groups of food	Gender	Examined no. rats
	#3	Fetus & New born	9
		Male	12
		Female	6
	#4	Fetus & New born	13
		Male	26
		Female	32
	#5	Fetus & New born	7
		Male	5
		Female	5
	#6	Fetus & New born	8
		Male	3
		Female	6
iv	#1	Male	8
		Female	5
	#2	Male	7
		Female	8
	#3	Male	4
		Female	6
	#4	Male	5
		Female	6
	#5	Male	4
		Female	10
	#6	Male	5
		Female	5
v	#1	Male	7
		Female	8
	#2	Male	7
		Female	8
	#3	Male	7
		Female	8
	#4	Male	9
		Female	17
	#5	Male	7
		Female	8
	#6	Male	7
		Female	7
Normal	Normal	Fetus & New born	122
		Male	45
		Female	65
			Total 827

Acta Neurochir. 2006 in press.

RESTITUTION OF ISCHEMIC INJURIES IN PENUMBRA OF CEREBRAL CORTEX AFTER TEMPORARY ISCHEMIA

Umeo Ito,[1,3] Eiko Kawakami,[1] Jun Nagasao,[1] Toshihiko Kuroiwa,[2] Imaharu Nakano,[3] and Kiyomitsu Oyanagi [1]

[1.] Dept. of Neuropathol., Tokyo Metropolitan Institute for Neuroscience, Tokyo, [2.] Dept. of Neuropathol., Medical Research Institute, Tokyo Medical and Dental University, Tokyo [3.] Dept. of Neurol., Jichi Medical School, Tochigi

Summary:

We investigated at both light and ultrastructural levels the fate of swollen astrocytes and remodeling of the neurites connected to disseminated dying neurons in the ischemic neocortical penumbra. Specimen were obtained from the left cerebral cortex cut coronally at the infundiblum and observed by light and electron microscopy. We measured the number of synapses and spines, and thickness of neuritic trunks in the neuropil on EMS photos. We also determined the percent volume of the axon terminals and spines by Weibel's point counting method. The astrocytic swelling gradually subsided from 4th day after the ischemic insult, with increases in cytoplasmic glial fibrils and number of GFAP positive astrocytes. The disseminated dying electron-dense neurons (eosinophilic ischemic neurons in light microscopy) had been fragmented by invading astrocytic cell processes and accumulated as granular pieces (eosinophilic ghost cells by light microscopic observation). The number of synapses and spines and the total percent volume of the axon terminals and spines decreased, and there was an increasing sparsity of synaptic vesicles until the 4th day. From 1 to 12 weeks after the ischemic insult, however, these values increased to or exceeded the control ones, and there were sprouting and an increase in the number of synaptic vesicles. Some of the axons attached to the dying neurons showed abnormal distension of their terminals, but most of the axon terminals were found around crusts of granular pieces of fragmented dead neurons. From 1 to 12 weeks, some axon terminals associated with crusts became newly connected to the spines and neurites of the surviving neurons. These axons shifted their connections to the spines and the thickened neurites of the surviving neurons. Astrocytic restitution and neuronal remodeling processes started 4 days and continued until 12 weeks after the ischemic insult.

Key Words: maturation phenomenon in cerebral ischemia, GFAP stained glial fibrils, eosinophilic ghost cells, scavenge of dead neuron, axons attached to the dead neurons, neuronal remodeling, spines and axon terminals, neurites

Introduction:

Cerebral infarction develops rapidly after a large ischemic insult. Earlier, we developed a model to induce a large ischemic penumbra around a small focal infarction in the cerebral cortex of Mongolian gerbils [5, 6] by giving a threshold amount of ischemic insult to induce cerebral infarction. The histopathology of this model revealed disseminated eosinophilic ischemic neurons by light microscopic observation, and disseminated electron-dense neurons seen ultrastructurally (disseminated selective neuronal necrosis:DSNN) increased in number in the penumbra of the cerebral cortex after restoration of blood flow. Then a focal infarction developed later in a part of this area of DSNN by 12~24 hours after the ischemic insult, due to massive astrocytic death. This area expanded gradually, involving dead and still living eosinophilic neurons, and normal- looking neurons involving to death until 4 days after the ischemic insult [6, 9, 11]. No additional new infarction (pan necrosis) was found later than 4-days after the ischemic insult, in our coronal as well as para-sagittal sections of the forebrain [3, 19].

In previous studies on the cortical penumbra [7, 9, 11], we found that the cytoplasm and the cell processes of living astrocytes in the penumbra were actively swollen and that brain edema, determined by tissue gravimetry, was maximum around 3 days after the ischemic insult and subsided gradually by 7 days after it [4, 9]. The isolated dark neurons with different grades of high-electron density increased in number among the normal-looking neurons from 5 to 24 hours. These dark neurons were surrounded by remarkably swollen astrocytic cell processes. As a general pathological sign of irreversible cellular damage, granular chromatin condensation was apparent in the nuclear matrix and along the nuclear membrane of some of these dark neurons [10]. The dark neurons increased in number rapidly until day 4, and new ones still appeared 12 weeks after the ischemic insult. Theses observations correspond to the maturation phenomenon of ischemic injuries [3, 12, 19], whichi is the same as the delayed neuronal death described for CA1 neurons [3, 15, 19].

In the present study, we investigated at the ultrastructural level the fate of swollen edematous astrocytes, and dead neurons and remodeling of the axons connected to the dead neurons in the ischemic penumbra.

Materials and Methods:

Stroke positive Mogolian gerbils were selected according to their stroke index score [18] during left carotid clipping of the Mongolian gerbils for 10 min., followed by another 10 min. clipping with 5 hour interval between two

occlusions. They were sacrificed at 5, 12, 24 hr, at 4 days, and at 3, 5, 8 ,12 and 24 weeks following the last ischemic insult by intracardiac perfusion with cacodylate-buffered glutaraldehyde fixative (3 animals in each group) for electron microscopy and with 10% phosphate-buffered formaldehyde fixative for light microscopy (5 animals in each group).

Ultrathin sections including the 2nd~5th cortical layers were obtained from the neocortex at the mid-point between the interhemispheric and rhinal fissures on the left coronal face sectioned at the infundibular level, in which only the penumbra appeared. The sections were double stained with uranyl acetate and lead solution, and observed with a Hitachi electron microscope (H9000). Separate paraffin sections were stained with hematoxylin-eosin (HE), periodic acid fuchsin Schiff (PAS) or by Bodian silver impregnation or immuno-histochemically for GFAP.

Placing 1 cm x 1 cm lattices on the 5,000 x 2.67 times enlarged EM photo-graphs we measured the number of synapses and spines in the neuropil in a 100-square cm (56 sq. μ, by real size), and determined the percent volume of the axon terminals (ATs) and spines(SPs) using the point counting method (Weibel 1963) [22] by counting intersections of the lattice dropped on the ATs and/or SPs. We also measured neuritic thickness as the maximal diameter perpendicular to their neurofilaments and / or microtubules, on the same EM pictures.

Results:

1. The astrocytic swelling gradually subsided starting on day 4 after the ischmeic insult, increased in the number of cytoplasmic glial fibrils in astrocytes observed ultrastructurally and GFAP positive cells seen light microscopically. Astrocytes in mitosis and/or with two nuclei were occasionally seen.

2. The disseminated dying electron dense neurons had been fragmented into granular pieces by invading astrocytic cell processes (Fig.1-A). These accumulations of the fragmented dark neurons were observed as eosinophilic ghost cells by light microscopy. These electron-dense granular pieces were dispersed around the extracellular spaces and phagocytized by microglias, astrocytes and neurons. There was no evidence of macrophages in the penumbra.

3. The number of synapses and spines, and the percent volume of the axon terminals and spines (Table) decreased with an increase in a sparsity of synaptic vesicles until the 4th day (Fig. 2-A). From 1 to 12 weeks after the ischemic

insult, however, they recovered to or exceeded the control values and were found surrounding the thickened neurites of the surviving neurons (Fig.2-B).

4 . From 4 days to 8 weeks after the ischemic insult, most of the axon terminals that had been attached to the dying neurons were found around the fragmented dead dark neurons. Some of them were separated from the dead neurons, being attached a crust of the granular electron dense fragments (Fig.1-A). From 24 hours to 8 weeks after the ischemic insult, some axons attached to the dying neurons showed globular or spindle-shaped distension of their terminals as seen by Bodian silver impregnation (Fig.1-B). EM observation of these distensions showed amplified axon terminals containing degenerated mitochondria, lamellated dense bodies, and irregularly located neurofilaments and microtubules. They were frequently observed around the accumulations of the fragmented electron-dense granular pieces of dead neurons.

5. From 1 to 12 weeks, some axon terminals associated with crusts of the electron dense granular pieces became newly connected to the spines and neurites of the surviving neurons.

6. Neuronal death still continued repeatedly in the penumbra during these periods (maturation phenomenon). From 8 to 24 weeks after the ischemic insult, these structures and the accumulation of eosinophilic ghost cells remained laminally confined to the 3rd cortical layer, especially in some portion of the lateral part of the left coronal face sectioned at the infundibular level. Cortical thickness and cortical neuronal density were reduced evenly in the face during these periods.

Discussion:

In the acute phase after an ischemic insult, astrocytes become swollen showing increases in the number of glycogen granules and mitochondrial size and number, indicating an active reaction of the astocytes to prevent ischemic neuronal injuries [7, 9]. However, later than 4 days after the ischemic insult, astrocytic swelling subsides and glial fibrils, stained by GFAP antibodies, increase in number. These GFAP positive reactive astrocytes are increased in number by mitotic division, especially those surrounding the focal infarction (pan necrosis), which evolves and developes from 12-hr to 4 days after ischemic insult. The infarcted necrotic tissue is then scavenged by macropghages and becomes liquefied thereafter [3, 6, 19]. The infarcted focus is surrounded by gliosis induced by reactive astrocytes. In the penumbra, GFAP-positive reactive astrocytes increase moderately in number,but do not induce gliosis. These are the restitutional processes of the astrocytes in the

damaged ischemic tissue.[6]

It has been thought that dead neurons and ischemically injured tissue are scavenged by macrophages invasion into the injured tissue from the blood stream. However, dead neurons were found disseminated among surviving neurons, in the present study, in the cortical penumbra. The axons and dendritic processes of the dying neurons were still connected to axon terminals and neurites of the surviving neurons. These solitary dying neurons, which were connected by neuritic networks, were not phagocytized by a single macrophage. Furthermore, in contrast to the case of infarction i.e., massive necrosis, macrophages did not enter the neuropil of the penumbra where the network of the neuropil was still tight. In this situation, it is reasonable that the shrunken dead neurons would become fragmented into granular debris (eosinophilic ghost cells seen by the light microscopy) and removed by astrocytes, neurons and perivascularly located microglias [8, 14, 16]. However, the tattered central cytosol of the shrunken neurons remained for more than 5 weeks. No inflammatory cells and macrophages appeared in the ischemic penumbra wandering among the neuropils. [8, 16]

In the entire neuropils of the ischemic penumbra in the cerebral cortex, we found a marked decrease in the number of the synapses and volume of the axon terminals from 5-hr to 4-days after the start of recirculation, along with a marked shrinkage of the axon terminals, which contained a decreased number of synaptic vesicles. These changes seemed to be due to calcium-dependent neuronal hyperexcitation [21] and were reduced by NMDA receptor antagonists in a morphological study recording EPSPs from hippocampal slice cultures subjected to brief anoxia-hypoglycemia [13].

From 1 to 12 weeks after the ischemic insult, the number of synapses increased gradually, associated with an increase in the volume of axon terminals showing sprouting [20] and paralleling the marked increase in the number of synaptic vesicles. Also, the number and volume of spines increased in parallel. The axons that had been attached to the dying neurons were considered to have shifted their connections to the spines and the neurites of the surviving neurons, increasing their thickness associated with synaptogenesis in the neuropil [1, 2, 17]. In the ischemic penumbra, the neuronal remodeling process progressed from its early stage to 12 weeks after the start of recirculation.

References:

1. Crepel V, Epsztein J, and Ben-Ari Y, Ischemia induces short- and long-term

remodeling of synaptic activity in the hippocampus, J Cell Mol Med, 2003. 7(4): p. 401-7.

2. Frost SB, Barbay S, Friel KM, Plautz EJ, and Nudo RJ, Reorganization of remote cortical regions after ischemic brain injury: a potential substrate for stroke recovery, J Neurophysiol, 2003. 89(6): p. 3205-14.

3. Graham DI and Lantos PL, Greenfield's Neuropathology. 2002. p. 230-280.

4. Hakamata Y, Hanyu S, Kuroiwa T, and Ito U, Brain edema associated with progressive selective neuronal death or impending infarction in the cerebral cortex, Acta Neurochir Suppl, 1997. 70: p. 20-2.

5. Hanyu S, Ito U, Hakamata Y, and Nakano I, Topographical analysis of cortical neuronal loss associated with disseminated selective neuronal necrosis and infarction after repeated ischemia, Brain Res, 1997. 767(1): p. 154-7.

6. Ito U, Hanyu S, Hakamata Y, Arima K, Oyanagi K, Kuroiwa T, and Nakano I. Temporal profile of cortical injury following ischemic insult just-below and at the threshold level for induction of infarction--light and electron microscopic study. in (eds.) Ito U, Fieschi C, Orzi F, Kuroiwa T, Klatzo I, Maturation Phenomenon in Cerebral Ischemia III. 1999: Springer-Verlag. pp.227-235

7. Ito U, Hanyu S, Hakamata Y, Nakamura M, and Arima K, Ultrastructure of astrocytes associated with selective neuronal death of cerebral cortex after repeated ischemia, Acta Neurochir Suppl, 1997. 70: p. 46-9.

8. Ito U, Kuroiwa T, Hakamata Y, Kawakami E, Nakano I, and Oyana K. How are ischemically dying eosinophilic neurons scavenged in the penumbra? An ultrastructural study. in (eds.) Krieglstein J, Klumpp S,Pharmacology of cerebral ischemia. 2002: medpharm Science Publication, Stuttgart. pp. 261-265

9. Ito U, Kuroiwa T, Hanyu S, Hakamata Y, Kawakami E, Nakano I, and Oyanagi K, Temporal profile of experimental ischemic edema after threshold amount of insult to induce infarction--ultrastructure, gravimetry and Evans' blue extravasation, Acta Neurochir Suppl, 2003. 86: p. 131-5.

10. Ito U, Kuroiwa T, Hanyu S, Hakamata Y, Kawakami E, Nakano I, and Oyanagi K. Ultrastructural temporal profile of the dying neuron and surrounding astrocytes in the ischemic penumbra:apoptosis or necrosis? in (eds.) Buchan AM, Ito U, Colbourne F, Kuroiwa T, Klatzo I Maturation Phenomenon in Cerebral Ischemia V. 2003,: Springer-Verlag, Berlin, Heidelberg. pp. 189-196

11. Ito U, Kuroiwa T, Hanyu S, Hakamata Y, Nakano I, and Oyanagi K, Ultrastructural behavior of astrocytes to singly dying cortical neurons., in Pharmacology of cerebral ischemia, In:(eds.) Krieglstein J and Klumpp Se, 2000, medpharm Science Publication: Stuttgart. p. 285-291.

12. Ito U, Spatz M, Walker J, Jr., and Klatzo I,Experimental cerebral ischemia in mongolian gerbils. I. Light microscopic observations, Acta Neuropathol Berl, 1975. 32(3): p. 209-23.

13. Jourdain P, Nikonenko I, Alberi S, and Muller D,Remodeling of hippocampal synaptic networks by a brief anoxia-hypoglycemia, J Neurosci, 2002. 22(8): p. 3108-16.

14. Kalmar-p-a B, Kittel A, Lemmens R, Kornyei Z, and Madarasz E,Cultured astrocytes react to LPS with increased cyclooxygenase activity and phagocytosis, Neurochem Int, 2001. 38(5): p. 453-61.

15. Kirino T, Tamura A, and Sano K,Delayed neuronal death in the rat hippocampus following transient forebrain ischemia, Acta Neuropathol Berl, 1984. 64(2): p. 139-47.

16. Lemkey-Johnston-p-a N, Butler V, and Reynolds WA,Glial changes in the progress of a chemical lesion. An electron microscopic study, J Comp Neurol, 1976. 167(4): p. 481-501.

17. Nudo RJ, Larson D, Plautz EJ, Friel KM, Barbay S, and Frost SB,A squirrel monkey model of poststroke motor recovery, Ilar J, 2003. 44(2): p. 161-74.

18. Ohno K, Ito U, and Inaba Y,Regional cerebral blood flow and stroke index after left carotid artery ligation in the conscious gerbil, Brain Res, 1984. 297(1): p. 151-7.

19. Rosenblum WI,Histopathologic clues to the pathways of neuronal death following ischemia/hypoxia, J Neurotrauma, 1997. 14(5): p. 313-26.

20. Stroemer RP, Kent TA, and Hulsebosch CE,Neocortical neural sprouting, synaptogenesis, and behavioral recovery after neocortical infarction in rats, Stroke, 1995. 26(11): p. 2135-44.

21. von Lubitz DK and Diemer NH,Cerebral ischemia in the rat: ultrastructural and morphometric analysis of synapses in stratum radiatum of the hippocampal CA-1 region, Acta Neuropathol (Berl), 1983. 61(1): p. 52-60.

22. Weibel ER, Morphometry of the human lung. 1963, Springeer-Verlag, Berlin,Gowttingen,Heidelberg. p. pp.19-20.

Legends of figures:

Fig. 1 A. EM picture of cerebral cortex 4-days after restoration of blood flow. The disseminated dying electron dense neuron has been fragmented into granular pieces by invading astrocytic cell processes. Some axon terminals that were attached to the dying neurons are found around the fragmented

dead dark neurons (arrow heads). Bottom bar 0.1 micron

B. LM picture of cerebral cortex 24-hr after restoration of blood flow. Some thick axons attached to the dying neurons showed globular or spindle-shaped distension of their terminals surrounding the dead neuron (arrows) . Bodian silver impregnation Bottom bar 2 micron

Fig. 2 A. EM picture of cerebral cortex 4-days after restoration of blood flow. The number of synapses and spines, and the volume of the axon terminals and spines decreased with the increase in sparsity of synaptic vesicles (arrows). Neurites (N) are degenerative. Electron-dense granular pieces are dispersed in the extracellular spaces of the neuropil (arrow heads). Bottom bar 0.1 micron

B. EM picture of cerebral cortex 12-W after restoration of blood flow. The number of synapses and spines, and the volume of the axon terminals and spines recovered, with increase in the number of synaptic vesicles (arrows). Neurites (N) are thickened surrounded and/or synapsed by axon terminals. Bottom bar 0.1 micron

Fig. 1A

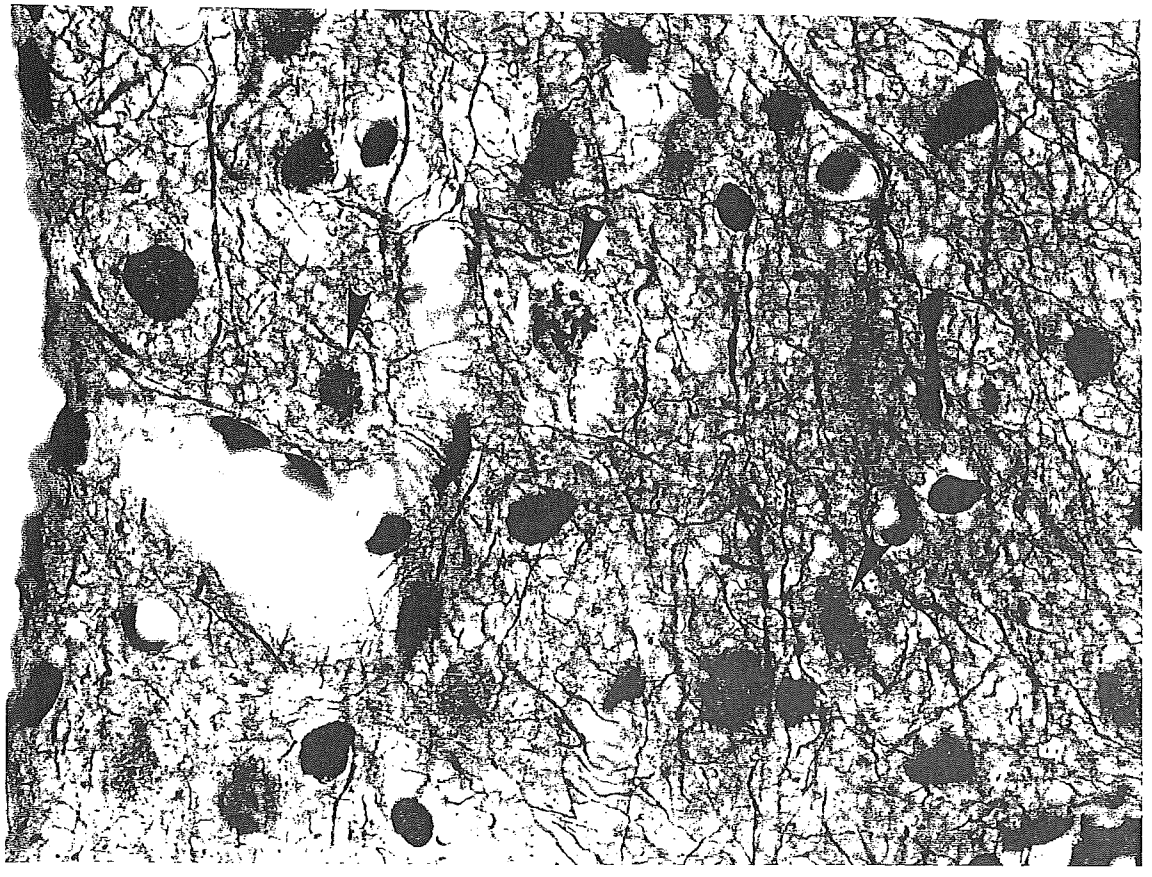

Fig. 1B

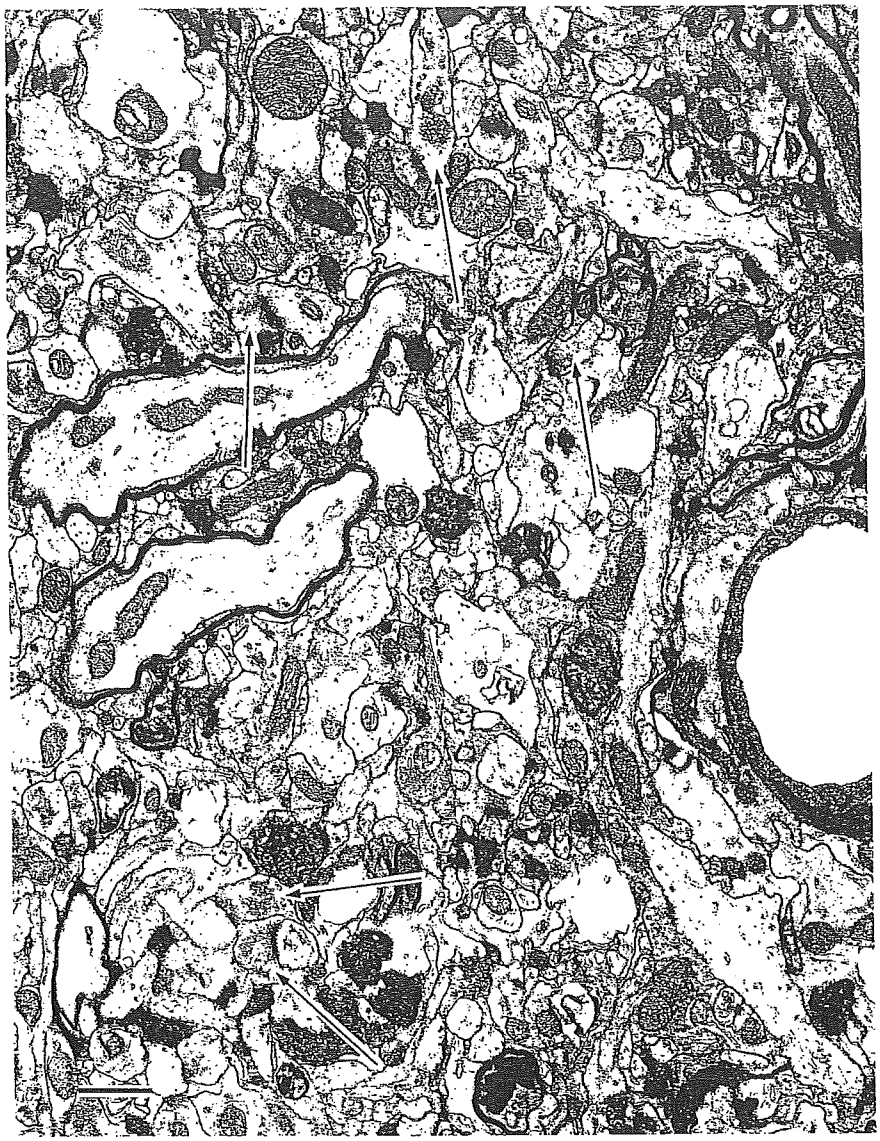

Fig. 2A

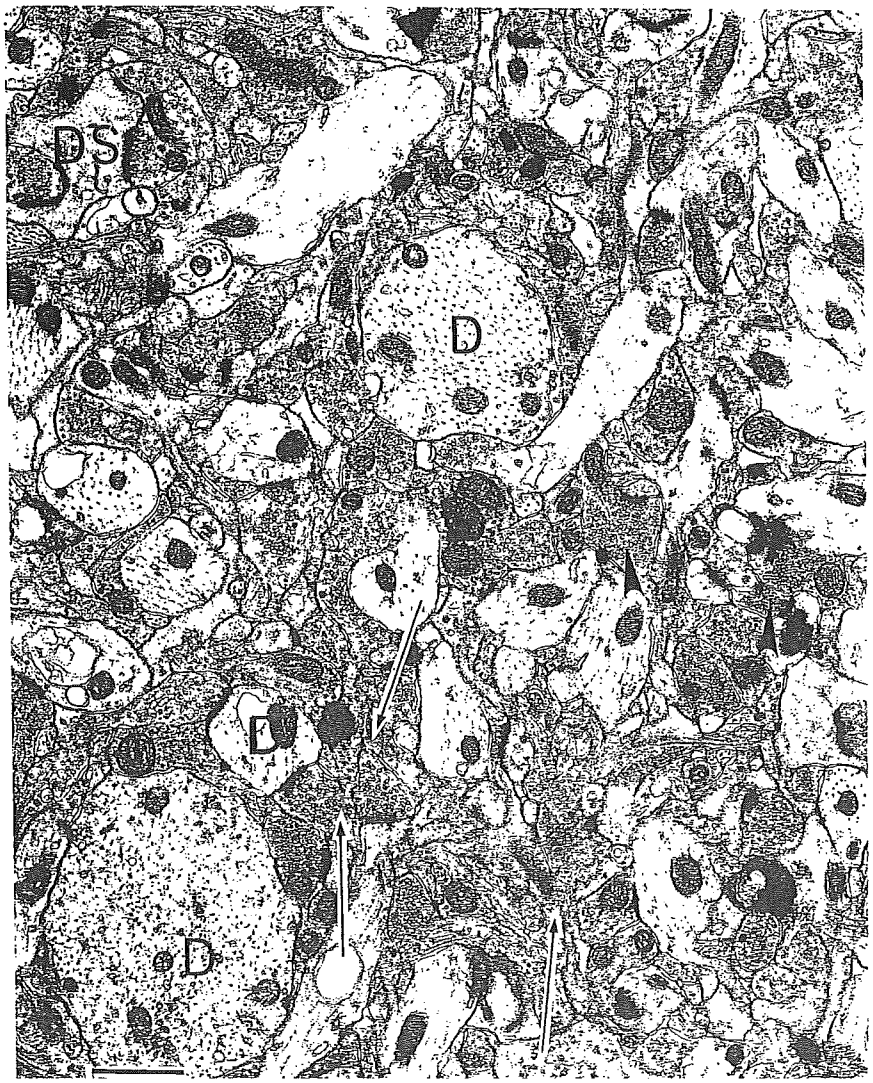

Fig. 2B

Transcriptional repression induces a slowly progressive atypical neuronal death associated with changes of YAP isoforms and p73

Masataka Hoshino,[1] Mei-ling Qi,[1] Natsue Yoshimura,[1] Tomoyuki Miyashita,[2] Kazuhiko Tagawa,[1] Yo-ichi Wada,[1] Yasushi Enokido,[1] Shigeki Marubuchi,[1] Phoebe Harjes,[3] Nobutaka Arai,[2] Kiyomitsu Oyanagi,[2] Giovanni Blandino,[4] Marius Sudol,[5] Tina Rich,[6] Ichiro Kanazawa,[7] Erich E. Wanker,[3] Minoru Saitoe,[2] and Hitoshi Okazawa[1,2,8]

[1]Department of Neuropathology, Medical Research Institute and Center of Excellence Program for Brain Integration and Its Disorders, Tokyo Medical and Dental University, Bunkyo-ku, Tokyo 113-8510, Japan
[2]Tokyo Metropolitan Institute for Neuroscience, Fuchu, Tokyo 183-8526, Japan
[3]Neuroproteomics, Max-Delbrück Center for Molecular Medicine, 13092 Berlin, Germany
[4]Department of Experimental Oncology, Regina Elena Cancer Institute, 00158 Rome, Italy
[5]Weis Center for Research, Geisinger Clinic, Danville, PA 17822
[6]Department of Pathology, University of Cambridge, Cambridge CB2 1QP, England, UK
[7]National Center for Neurology and Psychiatry, Kodaira, Tokyo 187-8502, Japan
[8]Precursory Research for Embryonic Science and Technology, Japan Science and Technology Agency, Kawagoe, Saitama 332-0012, Japan

Transcriptional disturbance is implicated in the pathology of polyglutamine diseases, including Huntington's disease (HD). However, it is unknown whether transcriptional repression leads to neuronal death or what forms that death might take. We found transcriptional repression-induced atypical death (TRIAD) of neurons to be distinct from apoptosis, necrosis, or autophagy. The progression of TRIAD was extremely slow in comparison with other types of cell death. Gene expression profiling revealed the reduction of full-length yes-associated protein (YAP), a p73 cofactor to promote apoptosis, as specific to TRIAD. Furthermore, novel neuron-specific YAP isoforms (YAPΔCs) were sustained during TRIAD to suppress neuronal death in a dominant-negative fashion. YAPΔCs and activated p73 were colocalized in the striatal neurons of HD patients and mutant huntingtin (*htt*) transgenic mice. YAPΔCs also markedly attenuated Htt-induced neuronal death in primary neuron and *Drosophila melanogaster* models. Collectively, transcriptional repression induces a novel prototype of neuronal death associated with the changes of YAP isoforms and p73, which might be relevant to the HD pathology.

Introduction

Neurodegenerative disorders are characterized by the slow exacerbation of symptoms and by gradual progression of brain pathologies. Patients suffer for 5–20 yr from the onset of the disease to the bed-ridden state. Even fast-progressing amyotrophic lateral sclerosis takes 2–5 yr to render the patient bed ridden. Regarding the pathology, the total number of neurons and neural networks among them decrease. However, some of the neurons survive for an extensive period of time despite their expression of abnormal structures that are derived principally from the pathogenic disease-causing products. Typically, nigral neurons that express Lewy bodies in Parkinson's disease, hippocampal neurons that carry paired helical filaments in Alzheimer's disease, and motor neurons bearing Bunina bodies in amyotrophic lateral sclerosis can partially survive until the death of the patient. The mutant protein aggregates that characterize many of these diseases are known to trigger multiple cellular responses, including ER stress and mitochondrial abnormality. These stress responses are clearly sufficient to induce apoptosis in nonneuronal cell lines, whereas the brain pathology of patients indicates that neurons survive for a long period before their demise. A lengthy period of cell death is also observed in the polyglutamine (polyQ) diseases, a major group of neurodegeneration that includes nine disorders (for reviews see Gusella and MacDonald, 2000; Zoghbi and Orr, 2000; Ross, 2002; Taylor et al., 2002; Bates, 2003). Again, a fraction of the neurons that possess nuclear and/or cytoplasmic inclusions of mutant

Correspondence to Hitoshi Okazawa: okazawa-tky@umin.ac.jp

Abbreviations used in this paper: AMA, α-amanitin; CDDP, cisplatin; FL-YAP, full-length YAP; HD, Huntington's disease; Pol II, polymerase II; polyQ, polyglutamine; siRNA, short inhibitory RNA; TRIAD, transcriptional repression-induced atypical death; YAP, yes-associated protein.

The online version of this article contains supplemental material.

The Journal of Cell Biology, Vol. 172, No. 4, February 13, 2006 589–604
http://www.jcb.org/cgi/doi/10.1083/jcb.200509132

Supplemental Material can be found at:
http://www.jcb.org/cgi/content/full/jcb.200509132/DC1

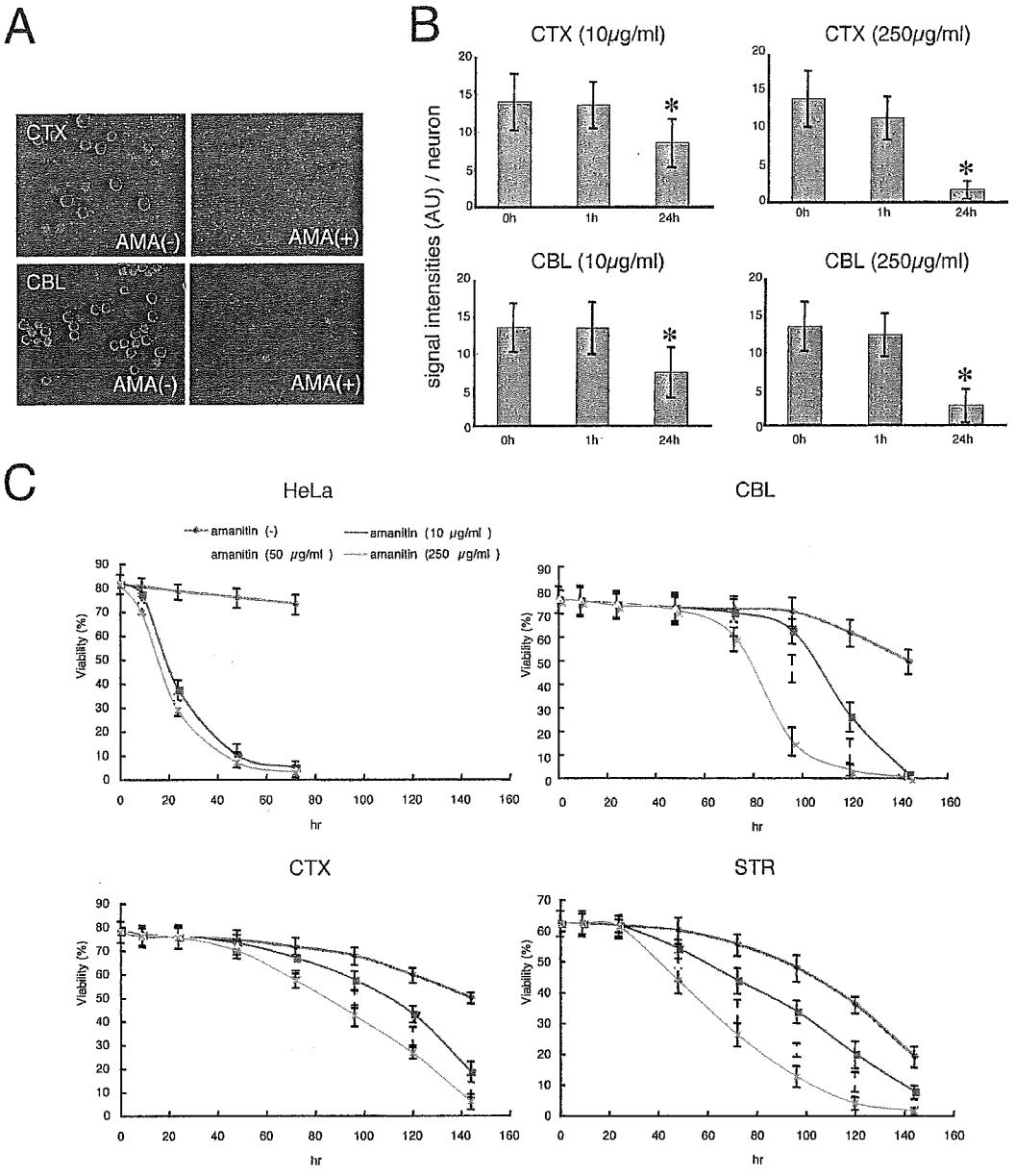

Figure 1. **Transcriptional repression by α-AMA induces a slowly progressive death of primary neurons.** (A) Uptake of BrdU in primary cortical (CTX) or cerebellar (CBL) neurons (Hoshino et al., 2004) was remarkably reduced at 6 h after the addition of 25 μg/ml AMA, indicating that AMA reduces transcription. (B) BrdU uptakes per neuronal nucleus at different concentrations of AMA (10 and 250 μg/ml) were analyzed chronologically. Signal intensities (AU, arbitrary unit) calculated with AQUACOSMOS (Hamamatsu) were obtained from >500 cells. Means ± SD are shown (error bars). Asterisks indicate significant reductions compared with 0 h ($P < 0.01$, *t* test). (C) Survival curves of HeLa cells and primary neurons (cortical, cerebellar, and striatal [STR] neurons) with AMA (10, 25, and 250 μg/ml). Viability (percent) indicates live cells/total cells by trypan blue assay (Tagawa et al., 2004) in six independent wells. Viability was shown as means ± SD of nonstained cells. Viability of HeLa cells declined at 24 h. In primary neurons, a significant reduction was first observed at 72 h at all concentrations of AMA. Of the three types of neuron tested, striatal neurons were the most vulnerable to AMA treatment for 48 h at 25 and 250 μg/ml AMA. $P < 0.05$ (*t* test).

polyQ peptides survives even in affected regions of the brain until the time of necropsy. So far, there is no model that fully explains the lengthy period of cell death in neurodegeneration.

In addition to ER and mitochondrial stresses, transcriptional dysfunction is suggested as a critical pathological component of polyQ diseases (for reviews see Gusella and MacDonald, 2000; Zoghbi and Orr, 2000; Ross, 2002; Taylor et al., 2002; Bates, 2003). Translocation of mutant proteins to the nucleus seems essential for neuronal dysfunction or cell death in polyQ diseases (Klement et al., 1998; Saudou et al., 1998; Katsuno et al., 2003). Numerous transcription-related factors, including LANP, PQBP-1, N-CoR, ARA24, p53, mSin3A, ETO/MTG8,

P160/GRIP1, A2BP1, $TAF_{II}130$, CA150, CRX, Sp1, CtBP, PML, $TAF_{II}30$, NF-κB, and SC35, are known to interact or colocalize with mutant polyQ disease proteins (for reviews see Okazawa, 2003; Sugars and Rubinsztein, 2003). Interaction with polyQ proteins may impair physiological functions of these transcription factors (Okazawa, 2003; Sugars and Rubinsztein, 2003), and, finally, even the general transcription level could be repressed (Hoshino et al., 2004). Some of these polyQ pathology-mediating factors bind directly to the core of transcription machinery, RNA polymerase II (Pol II; Okazawa et al. 2002). Therefore, one of the paramount issues in the field of polyQ diseases is the relationship between transcriptional dysfunction and neuronal death. However, as yet, the role of transcriptional disruption in neuronal death is unclear, as is the mode of neuronal death when transcription is severely impaired.

In this study, we found that inhibition of Pol II–dependent transcription leads neurons to undergo a slowly progressive atypical cell death (transcriptional repression-induced atypical death [TRIAD]) distinct from apoptosis, necrosis, or autophagy in morphological and biochemical analyses. Transcriptome analysis of TRIAD suggested that yes-associated protein (YAP), a known transcriptional cofactor, might be relevant to the death process. YAP, which was originally found as a binding protein to Src homology domain 3 of the yes proto-oncogene product (for review see Sudol et al., 1995), acts as a transcriptional cofactor of p73, mediates the expression of cell death–promoting genes, and induces apoptosis (Yagi et al., 1999; Basu et al., 2003; Melino et al., 2004). We found that in TRIAD, full-length YAP (FL-YAP) is down-regulated, and novel neuron-specific YAPΔC isoforms lacking the cell death–promoting activity sustain to protect neurons in a dominant-negative manner. The shift of balance in YAP isoforms seemed to slow down the cell death signaling pathway of p73 activated by α-amanitin (AMA), at least partially. We further questioned the relevance of YAP and p73 to Huntington's disease (HD) by using cellular, *Drosophila melanogaster*, and mouse models as well as human brain samples. Our data suggest that these molecules might be involved in neuronal death triggered by mutant Htt, the causative gene product of HD.

Results

Transcriptional repression induces an atypical slow neuronal death

To address the role of transcriptional disruption in neuronal death, we first made multiple short inhibitory RNAs (siRNAs) against RNA Pol II to suppress Pol II–dependent transcription. However, suppression of Pol II was inadequate and reminiscent of recent efforts to suppress basic transcription machinery by similar approaches (Ni et al., 2004). Therefore, we used a specific inhibitor of Pol II (AMA) whose three-dimensional molecular structure is exactly complementary to the groove of Pol II, through which mRNA is elongated (Cramer et al., 2001; Bushnell et al. 2002). Different concentrations of AMA were added to the culture medium of HeLa cells, primary rat embryonic (embryonic day [E] 15) cortical neurons, rat E15 striatal neurons, and rat pup cerebellar neurons (postnatal day [P] 7). BrdU up-take assay (Hoshino et al., 2004) showed significant repression of transcription at 6 h of AMA treatment in primary neurons (Fig. 1, A and B) and HeLa cells (not depicted). The survival of AMA-treated cells estimated by trypan blue assay (Fig. 1 C) revealed that AMA induces a slowly progressive cell death in a dose-dependent fashion. This was most pronounced in primary neurons, with half-lives of nearly 5 d. AMA-induced neuronal death was much slower than low potassium–induced apoptosis of cerebellar neurons, whose half-life was ~12 h (not depicted). The slow progression of AMA-induced neuronal death was confirmed independently by MTT (3-[4, 5-dimethylthiazol-2-yl]-2, 5-diphenyltetrazolium bromide) assay (Fig. S1, available at http://www.jcb.org/cgi/content/full/jcb.200509132/DC1).

A population of HeLa cells (10–30%) began to show cytoplasmic vacuoles proximal to the nucleus (Fig. 2 A, HeLa-TRIAD) from 6–12 h after the addition of AMA. Similar vacuoles were also observed in cortical neurons treated with AMA for 2 d (Fig. 2 A, CTX neuron-TRIAD), although with a diminished frequency (1–5%). It is important to note that the vacuoles did not possess double-membrane structures reminiscent of autophagosomes. No classic apoptotic features such as chromatin condensation, nuclear fragmentation, or apoptotic bodies (Okazawa et al., 1996) were found in these neurons by electron microscopic analysis (Fig. 2 A). In addition, no necrotic features such as mitochondrial dilatation (Fig. 2 A, CTX neuron necrosis) or cytoplasmic ballooning and rupture (Fig. 2 A, CTX neuron necrosis) were observed in primary neurons under TRIAD.

Immunohistochemical analyses using organelle-specific antibodies excluded the idea that the cytoplasmic vacuole was derived from the Golgi apparatus, endosome, lysosome, and mitochondria (Fig. S2, available at http://www.jcb.org/cgi/content/full/jcb.200509132/DC1). Autophagosomes induced by rapamycin and labeled with EGFP-LC3, a marker protein of the autophagosome (Fig. 2 B, top and middle), failed to colocalize with AMA-induced vacuoles (Fig. 2 B, bottom). In addition, the size of AMA-induced vacuoles was larger than that of autophagosomes (Fig. 2 B, bottom). EGFP-LC3 actually expresses the LC3 peptide (Fig. 2 C, arrow), verifying the morphological result. Note that the immunoblot shows a nonspecific band that is consistently detected by this antibody (Fig. 2 C, asterisk; unpublished data). Furthermore, the addition of rapamycin to the medium increased LC3-positive vacuoles but did not affect the formation of LC3-negative vacuoles induced by AMA (Fig. S3 A). Collectively, these data suggested that AMA-induced cell death is distinct from autophagy. Finally, we found colocalization of the vacuoles with ECFP-ER fusion constructs (expressing calreticulin ER-targeting sequences and KDEL ER retrieval tags at the 5′ and 3′ ends, respectively, of ECFP; Fig. 2 D). It suggested that vacuoles might be derived from expanded ER.

In agreement with the absence of morphological features of apoptosis, genomic DNA analyses of cell lines and primary neurons did not show ladder formation after AMA treatment (Fig. 3 A). Caspase-3, -7, and -12 were not remarkably activated in primary neurons by AMA (Fig. 3 B). AMA induced neither the release of cytochrome c into the cytosol from these neurons (Fig. 3 C) nor the interaction of annexin-V with the membrane of these neurons at an early stage (Fig. S3 B). Caspase inhibitors

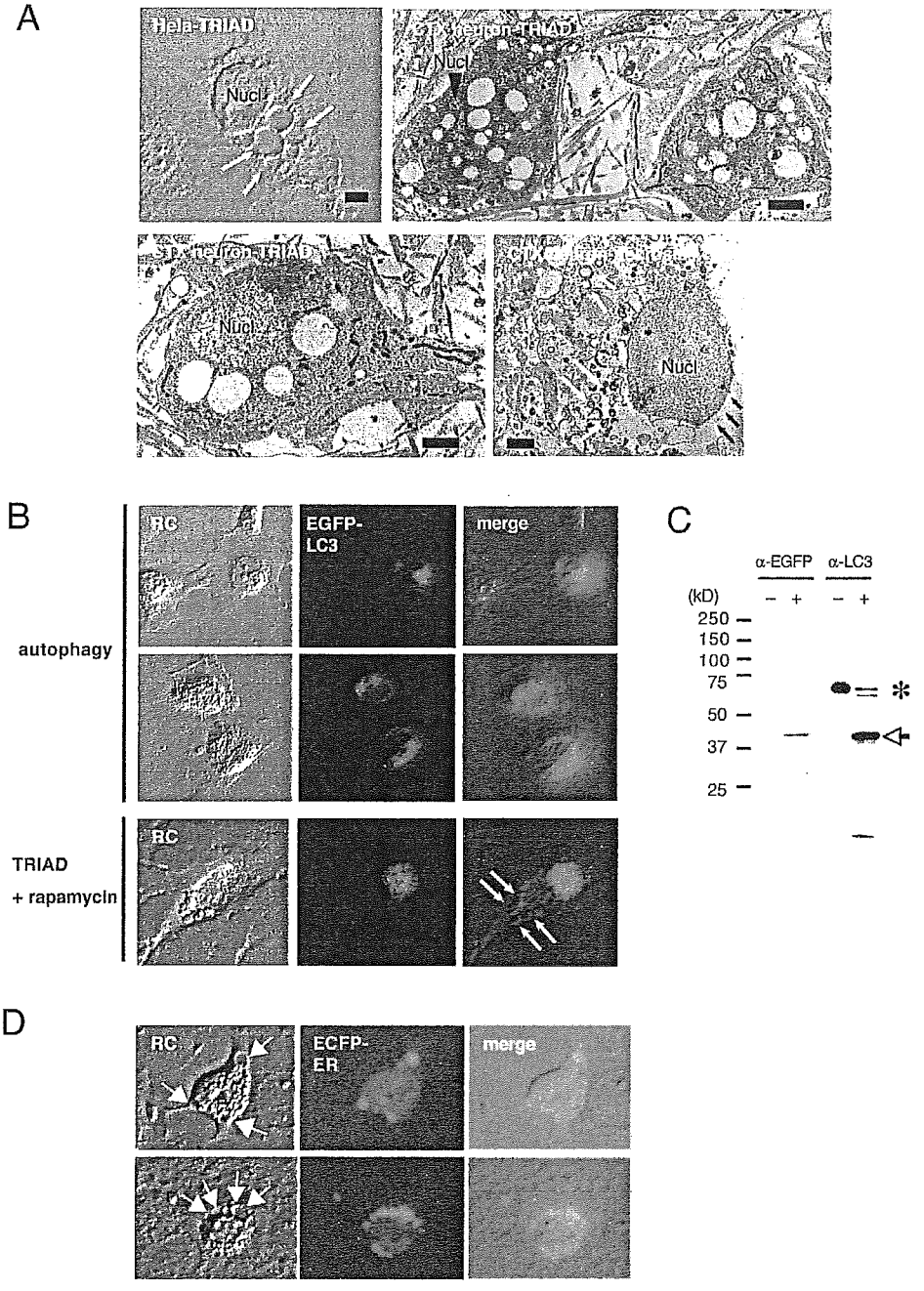

Figure 2. **Morphological features of TRIAD are distinct from those of apoptosis, necrosis, and autophagy.** (A) 10–30% of HeLa cells treated with 25 μg/ml AMA for 24 h (HeLa-TRIAD) showed cytoplasmic vacuoles (white arrows) proximal to the nucleus (Nucl). Electron microscopic analysis of cortical neurons treated with 25 μg/ml AMA for 48 h (CTX neuron TRIAD) revealed similar cytoplasmic vacuoles. Absence of chromatin condensation or nuclear fragmentation distinguishes TRIAD from classical apoptosis. The normal cytoplasm or mitochondria also excludes typical necrosis (bottom left). Electron microscopic analysis of primary cortical neurons in necrosis after freeze-thaw treatment (CTX neuron necrosis) showed the dilation of mitochondria (white arrows) and the rupture of cytoplasm (black arrows). Bars, 1 μm. (B) HeLa cells treated with 200 ng/μl rapamycin for 2 h showed autophagy (top and middle). AMA-induced vacuoles (arrows) did not merge with EGFP-LC3–labeled autophagosomes (bottom). RC, relief contrast. (C) Western blots to verify that pEGFP-LC3 expresses the LC3 peptide. Both anti-EGFP and anti-LC3 antibodies detect EGFP-LC3 (arrow), confirming that the EGFP-LC3 fusion protein is properly expressed. Asterisk indicates a nonspecific band. (D) A marker protein of ER, ECFP-ER (blue), was localized to AMA-induced vacuoles (arrows), suggesting that the vacuoles originate from the ER.

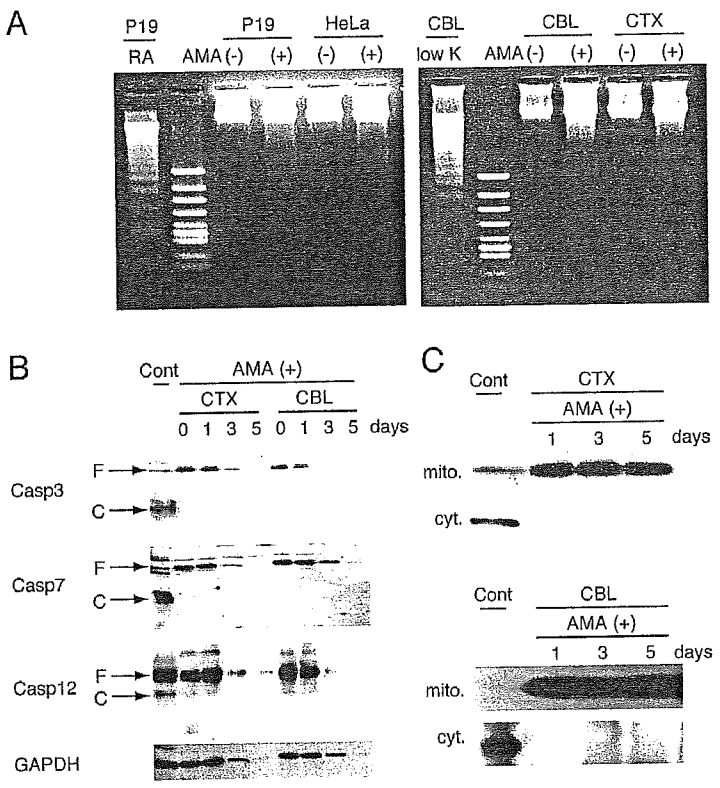

Figure 3. **Biochemical features of TRIAD are distinct from those of apoptosis.** (A) No significant fragmentation of genomic DNA was observed in TRIAD of P19 cells, HeLa cells, primary cerebellar neurons (CBL), and primary cortical neurons (CTX). Genomic DNA was prepared from total (attached and floating) cells cultured with 50 μg/ml AMA for 5 d. As controls of apoptosis, genomic DNA from P19 cells treated with 0.5 μM retinoic acid for 2 d or from cerebellar neurons cultured in a low potassium condition for 2 d were used. RA, retinoic acid. (B) Caspase-3, -7, and -12 were not remarkably activated in cortical and cerebellar neurons treated with 50 μg/ml AMA. Western blots were performed with antibodies specific for each caspase. F and C, full-length and cleaved forms, respectively. (C) No cytochrome c release in cytosol was observed in primary neurons treated with AMA. Mitochondrial (mito) and cytosol (cyt) fractions were prepared from primary cortical or cerebellar neurons treated with 50 μg/ml AMA for 1–5 d and blotted with anticytochrome c antibody.

z-DEVD-fmk and z-VAD-fmk did not repress AMA-induced cell death in neurons or in HeLa cells (not depicted). As expected, cycloheximide did not affect the cell death (not depicted). Calpain inhibitors, including ALLN and ALL, showed no remarkable effect on cell death. Pretreatment of cells with different concentrations of ATP in the medium did not affect AMA-induced cell death (not depicted).

Although AMA is a highly specific inhibitor of Pol II, as confirmed by molecular structural analyses (Cramer et al., 2001; Bushnell et al. 2002), to further verify that AMA-induced cell death is mediated by transcriptional repression, we examined the effect of another type of transcription inhibitor, actinomycin D, on primary neurons (Fig. S4, available at http://www.jcb.org/cgi/content/full/jcb.200509132/DC1). Actinomycin D binds directly to DNA and inhibits transcription (Jones, 1976) by stalling the rapidly moving fraction of Pol II (Kimura et al., 2002). We found that actinomycin D also induced a slowly progressive neuronal death (Fig. S4 A), in which some neurons show cytoplasmic vacuoles similar to those by AMA (Fig. S4 B). Neither DNA fragmentation nor caspase activation was induced by actinomycin D (Fig. S4, C and D). Collectively, our results suggest that AMA induces a slowly progressive TRIAD of neurons that is distinct from apoptosis, necrosis, and autophagy.

Novel YAP isoforms are expressed in neurons specifically

To understand the molecular basis of TRIAD, we conducted microarray analysis and compared gene expression profiles between TRIAD and low potassium–induced apoptosis in primary neurons. To detect initial changes, neurons were harvested at 1 h for RNA preparation. Duplicate experiments allowed us to extract eight genes whose expression levels changed in both apoptosis and TRIAD and a further 11 genes whose expression was changed specifically in TRIAD (Fig. 4 A). The latter group included YAP (Fig. 4 B), a transcriptional coactivator of p73 mediating apoptosis (Basu et al., 2003). Detailed information of the selected genes is provided in Fig. S5 (available at http://www.jcb.org/cgi/content/full/jcb.200509132/DC1). Northern blotting confirmed that AMA treatment down-regulates YAP expression at the level of transcription (Fig. 4 C).

Surprisingly, however, we identified novel isoforms of YAP containing 13-, 25-, and 61-nt inserts (Fig. 4, D and E) in addition to the full-length form by PCR cloning with RNA extracted from nontreated normal cortical and cerebellar neurons. The insert sequences matched genomic sequence with consensus junction sequences (Fig. 5). All three insertions lead to a reading frame shift, causing truncation of the COOH-terminal transcriptional activation domain (Fig. 4, D and E; Yagi et al., 1999). Therefore, we designated them YAPΔCs. Tissue expression profiling by RT-PCR revealed that the 13- and 61-nt insert isoforms (denoted here as Ins13 and Ins61, respectively) relatively specific to neurons (Fig. 4 F). Brain tissue (Fig. 4 F, third lane; not CTX or CBL neurons), including many glial and nonneuronal cells, showed only faint signals of the 13-nt variant comparable with those seen in other tissues (Fig. 4 F). Ins61 was highly specific to cortical neurons (Fig. 4 F). The 25-nt insert could not be detected by RT-PCR. Supporting the expression

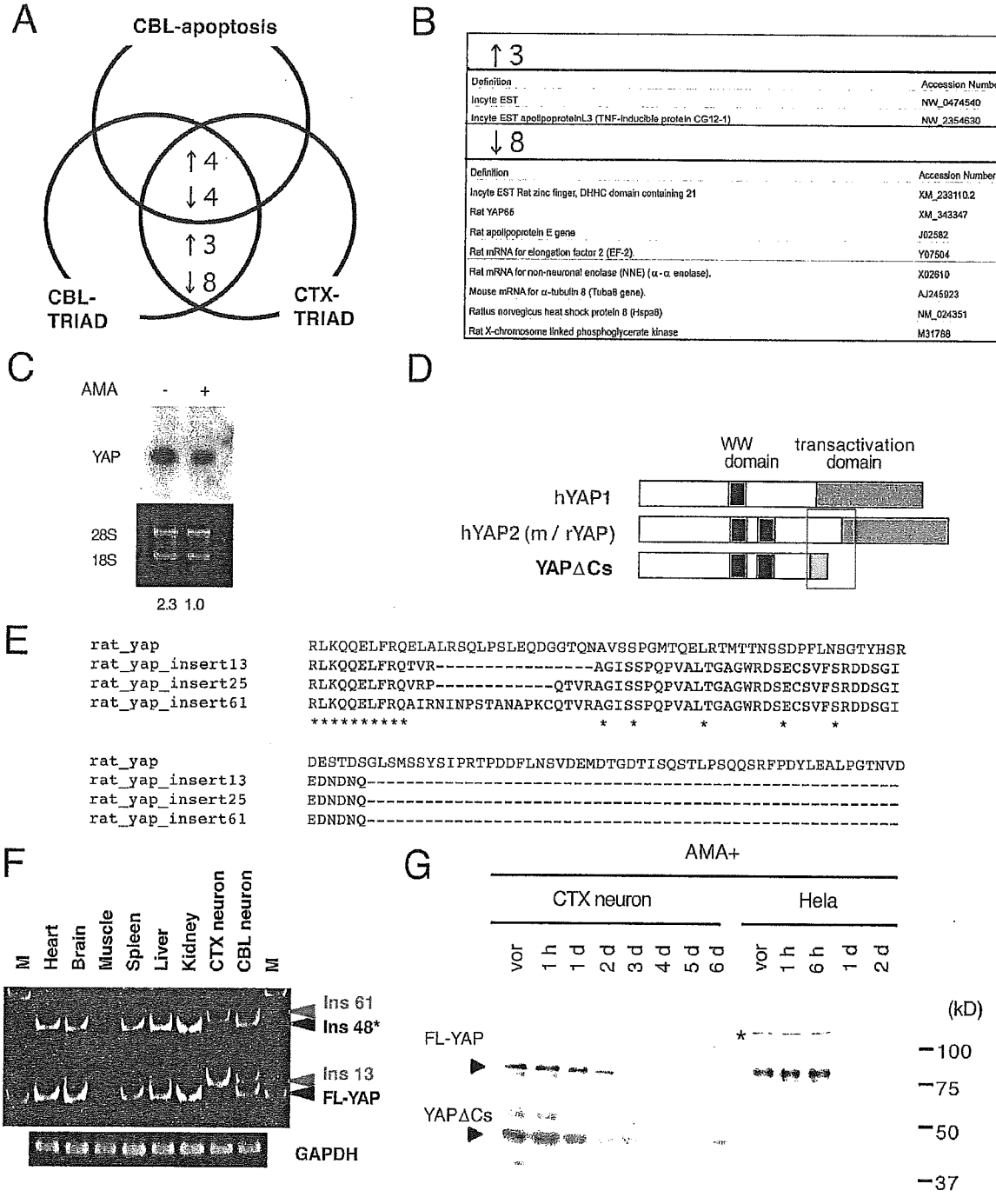

Figure 4. **Molecular features specific to TRIAD include YAP.** (A) Comparison of gene expression profiles among low potassium–induced apoptosis of cerebellar neurons, TRIAD of cerebellar neurons, and TRIAD of cortical neurons. Three genes were up-regulated, and eight genes were down-regulated specifically in TRIAD. (B) Genes specifically changed in TRIAD. (C) Down-regulation of YAP at 1 h after the addition of 25 μg/ml AMA was confirmed by Northern blotting. The bottom numbers indicate the signal intensities of the bands after correction with the 28S controls. (D) PCR cloning of YAP from primary neurons revealed new isoforms lacking the COOH-terminal transactivation domain (YAPΔCs). The scheme shows structures of YAPΔCs, mouse/rat fFL-YAP (m/rYAP = human YAP2), and human YAP1 (hYAP1). (E) Amino acid sequences of YAPΔCs around the junction (boxed area of D). Asterisks indicate conserved amino acids in four isoforms. (F) RT-PCR analysis of tissue-specific expression of YAPΔC isoforms. In addition to YAPΔCs, we detected full-length YAP (FL-YAP) and a previously reported isoform possessing a 48-bp insertion that does not cause a frame shift (ins48). YAPΔCins25 containing a 25-bp insert was not detected in this analysis. M, molecular weight marker. (G) Western blots showing chronological expression of YAP isoforms during TRIAD. In primary cortical neurons (CTX), the expression of YAPΔCs was sustained for 6 d after AMA addition, whereas FL-YAP was repressed within 2 d. Notably, the expression of YAPΔCs was very low in HeLa cells. The asterisk indicates an undetermined band whose expression was correlated with YAP. Vor, before the addition of AMA.

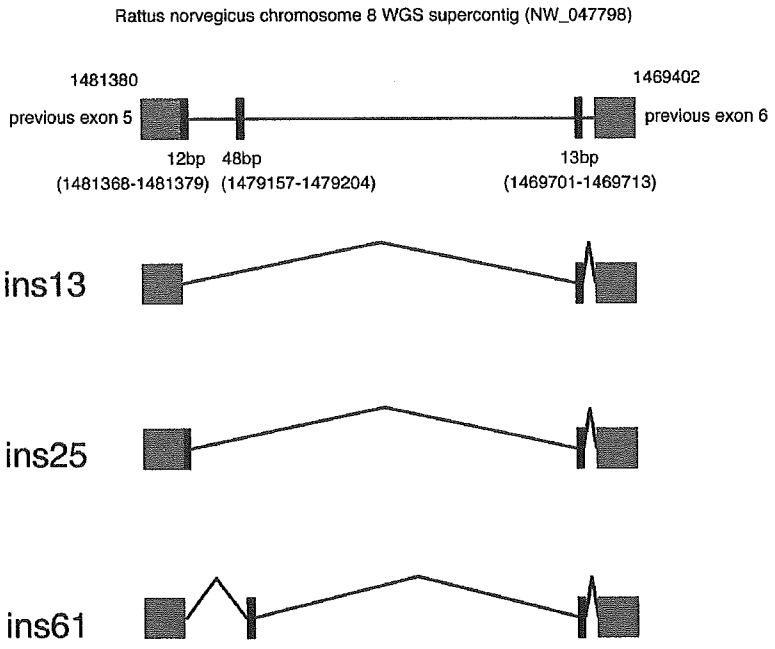

Figure 5. **Genomic structures of YAPΔC isoforms.** Genomic sequence numbers are derived from rat chromosome 8 supercontig. cDNA nucleotide sequences of novel YAP isoforms are available from GenBank/EMBL/DDBJ accession no. DQ186896, DQ186897, and DQ186898. Gray and black boxes are exons; black boxes indicate exons that were newly identified in this study.

of YAPΔCs in neurons, a truncated YAP isoform–specific antibody stained cortical and striatal neurons in immunohistochemistry with human and mouse brains (see Figs. 8 and 9).

In addition, temporal regulation of YAP isoforms during TRIAD was observed by Western blot analysis. Interestingly, although FL-YAP decreased before day 3 in cortical neurons, YAPΔCs were expressed at a relatively constant level (Fig. 4 G). It is also important to note that the levels of YAPΔCs were significantly lower in HeLa cells (Fig. 4 G). These data prompted us to test the function of YAP isoforms in TRIAD.

YAP isoforms modulate TRIAD

p73 and YAP mediate cisplatin (CDDP)-induced apoptosis of a cancer cell line, MCF-7 cells (Basu et al., 2003). In this case, DNA damage induced by CDDP leads to activation of p73, and the transcription cofactor YAP promotes p73-mediated transactivation of cell death genes, including Bax and possibly PUMA (Melino et al., 2004). Truncation of the transcriptional activation domain (Yagi et al., 1999) in YAP may impede transduction of the cell death stimulus, and YAPΔCs may act as dominant negatives against FL-YAP. As expected, luciferase assay showed that expression of YAPΔC isoforms represses p73-mediated activation of the p21/WAF1 gene promoter in MCF-7 cells by CDDP (Fig. 6 A, left; Basu et al., 2003). Overexpression of FL-YAP did not promote transcriptional activation any more (Fig. 6 A) probably because the function of endogenous FL-YAP was saturated. YAPΔCs also showed repressive effects on CDDP-induced apoptosis of MCF-7 cells (Fig. 6 B) mediated by FL-YAP (Basu et al., 2003). In these assays, the expression of each truncate was confirmed in parallel (Fig. 4, A and B; right).

Next, we tested whether YAPΔCs could repress TRIAD of primary cortical neurons (Fig. 6 C). Before the addition of AMA, neurons were infected with adenovirus vectors for YAPΔCs or the empty adenovector (AxCA) as a negative control (Fig. 6 C, left). Expression of YAPΔCs was confirmed by Western blot analysis simultaneously (Fig. 6 C, right). To further test whether YAPΔCs are involved in TRIAD, we transfected a siRNA targeting a sequence shared by three YAPΔC isoforms but not FL-YAP (Fig. 6 D). The siRNA accelerated TRIAD to ~90% (Fig. 6 D), supporting the idea that YAPΔCs suppress the cell death process in TRIAD at least partially.

The suppression of TRIAD by YAPΔCs suggested, in turn, that p73, the target transcription factor of FL-YAP, would be activated in TRIAD. Therefore, we analyzed the amount and phosphorylation of p73 in AMA-treated cortical neurons at day 2. As expected, AMA accelerated the phosphorylation of p73, whereas the total amount of p73 was not changed (Fig. 6 E). Together with the former results, YAPΔCs might inhibit the action of p73, leading neurons to apoptosis by antagonizing FL-YAP, especially at the early phase of TRIAD when FL-YAP is still expressed (Fig. 4 G).

Relevance of YAP isoforms and p73 to HD pathology

To investigate the relevance of YAP isoforms to the HD pathology, we infected primary cortical neurons with adenovirus vectors of YAPΔCs and found that expression of the truncated isoforms repressed Htt111-induced cell death of cortical neurons at 4 d after the infection of adenovirus vectors (Fig. 7 A; Tagawa et al., 2004). Consistently, YAPΔC-specific siRNA promoted Htt-induced cell death of cortical neurons (Fig. 7 B). We also found that mutant Htt induced p73 phosphorylation in cortical neurons at 2 d after infection (Fig. 7 C). Suppression of p73 by siRNA repressed cell death of mutant Htt-expressing neurons at day 4 (Fig. 7 D), suggesting the relevance of p73 to Htt-induced neuronal death. To examine the possible involvement of p73

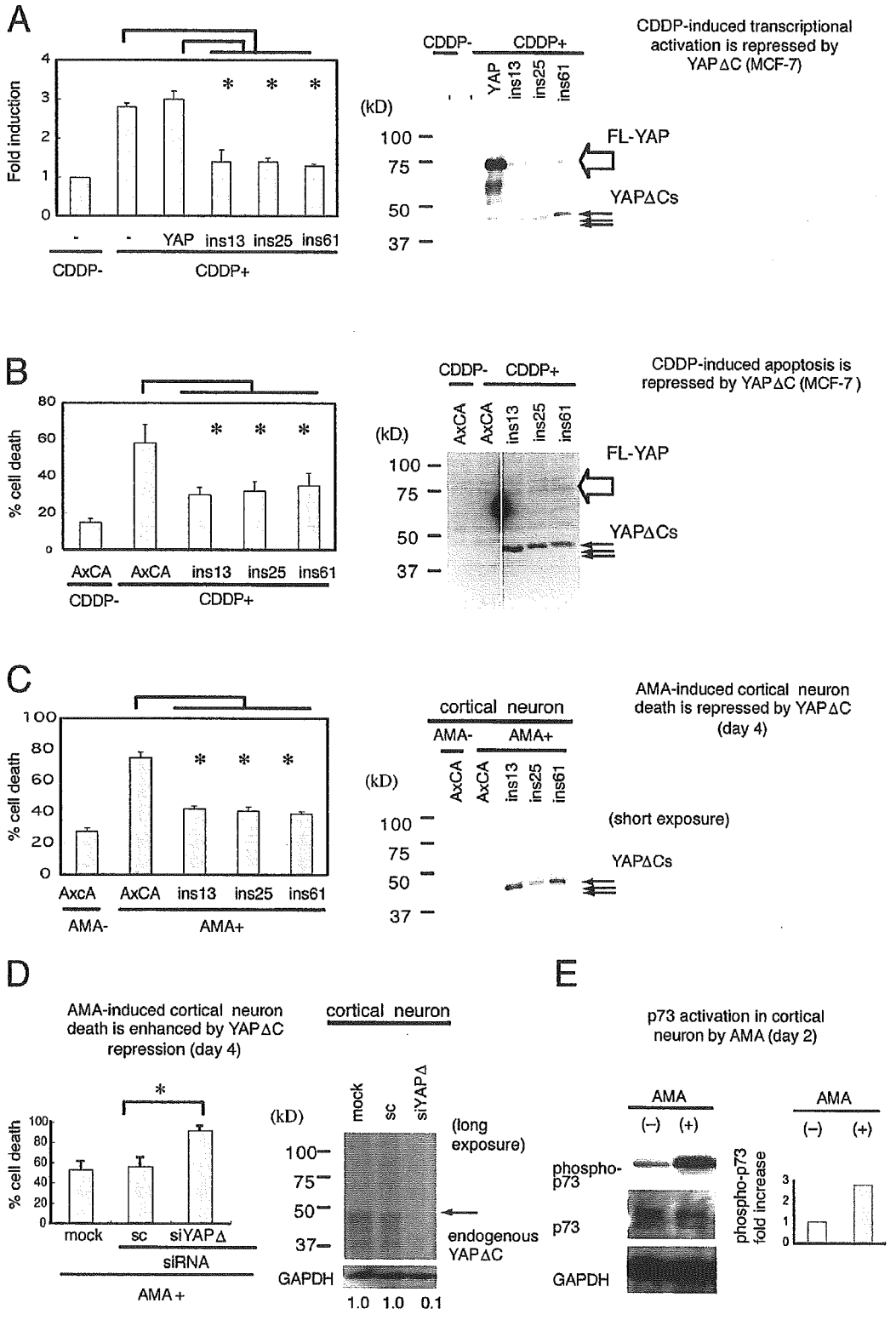

Figure 6. **YAPΔC isoforms repress apoptosis and the TRIAD.** (A) p73-mediated transcriptional activation by cisplatin (CDDP) was repressed by YAPΔCs. Luciferase assays were performed with MCF-7 cells 24 h after transfection of a p21/WAF1 reporter plasmid containing the p73 consensus cis-element and a YAPΔC expression vector (left). 25 μM CDDP was added 2 h after transfection. CDDP increased the transcription level to about threefold. Expression of YAPΔC isoforms (ins13, ins25, and ins61) remarkably repressed transcriptional activation by CDDP. FL-YAP (YAP) did not enhance the transcriptional activation, suggesting that endogenous YAP function was saturated. The expression of YAPs was checked simultaneously (right). $n = 6$. (B) YAPΔCs suppressed